Available online at www.sciencedirect.com

SciVerse ScienceDirect

Journal of Nutritional Biochemistry 23 (2012) 1417 – 1424

Journal of Nutritional Biochemistry

Adipose tissue proteomes of intrauterine growth-restricted piglets artificially reared on a high-protein neonatal formula☆,☆☆

Ousseynou Sarr, Isabelle Louveau, Isabelle Le Huërou-Luron, Florence Gondret*

INRA, UMR1079 Systèmes d'Elevage Nutrition Animale et Humaine, F-35590 Saint-Gilles, France
Agrocampus Ouest, UMR1079 Systèmes d'Elevage Nutrition Animale et Humaine, F-35000 Rennes, France

Received 3 January 2011; received in revised form 6 September 2011; accepted 8 September 2011

Abstract

The eventuality that adipose tissues adapt to neonatal nutrition in a way that may program later adiposity or obesity in adulthood is receiving increasing attention in neonatology. This study assessed the immediate effects of a high-protein neonatal formula on proteome profiles of adipose tissues in newborn piglets with intrauterine growth restriction. Piglets (10th percentile) were fed milk replacers formulated to provide an adequate (AP) or a high (HP) protein supply from day 2 to the day prior weaning (day 28, $n=5$ per group). Adipocytes with small diameters were present in greater proportions in subcutaneous and perirenal adipose tissues from HP piglets compared with AP ones at this age. Two-dimensional gel electrophoresis analysis of adipose tissue depots revealed a total of 32 protein spots being up- or down-regulated ($P<.10$) for HP piglets compared with AP piglets; 18 of them were unambiguously identified by mass spectrometry. These proteins were notably related to signal transduction (annexin 2), redox status (peroxiredoxin 6, glutathione *S*-transferase omega 1, cyclophilin-A), carbohydrate metabolism (ribose-5-phosphate dehydrogenase, lactate dehydrogenase), amino acid metabolism (glutamate dehydrogenase 1) and cell cytoskeleton dynamics (dynactin and cofilin-1). Proteomic changes occurred mainly in dorsal subcutaneous adipose tissue, with the notable exception of annexin 1 involved in lipid metabolic process having a lower abundance in HP piglets for perirenal adipose tissue only. Together, modulation in those proteins could represent a novel starting point for elucidating catch-up fat growth observed in later life in growing animals having been fed HP formula.

Keywords: Adipose tissue; Annexins; Low birth weight; Proteomics; Piglet; High-protein formula

1. Introduction

It is now recognized that nutrition imbalance during early life can affect the development of body tissues and confers a greater susceptibility to chronic disease in adulthood [1]. Epidemiological studies have hypothesized that babies born with intrauterine growth retardation (IUGR) may be at a greater risk of developing obesity, type 2 diabetes and hypertension later in life [2,3]. Those babies are often fed neonatal formula enriched in proteins to accelerate their weight gain [4,5]. However, a high protein intake during early life is also suspected to increase the risk of subsequent obesity [6–8]. Therefore, early nutrition may modulate the physiology of various tissues in a way that promotes short-term survival but that leads to a maladapted phenotype in later life.

White adipose tissues are expandable energy reserves and secretory organs that release numerous factors capable of regulating several physiological processes. Visceral adipose tissue is generally more strongly associated with an adverse metabolic risk profile than the subcutaneous adipose tissue in humans [9]. In an IUGR piglet artificially nourished with a high-protein milk replacer, Morise et al. [10] have recently reported a lower relative mass of perirenal adipose tissue at the day of weaning when compared with piglets fed formula with an adequate protein level. The mechanisms underlying short-term adaptations of adipose tissues to early postnatal protein nutrition have been however poorly investigated. To date, lower expression of glucose transporters (GLUT4) have been demonstrated on abdominal adipocyte cell membranes of artificially reared infant rats with high protein intakes [11]. Based on a bottom-up approach using 2-dimensional polyacrylamide gel electrophoresis (2DE) followed by mass spectrometry (MS) protein identification technology, recent studies have shown tissues-specific modulation of various proteins notably involved in intermediary metabolism, protein turnover, immune function or cell growth in response to IUGR in porcine neonates [12,13]. This suggests that 2DE analysis of key tissues may add new information to better understand nutrition-associated problems in animals and humans, such as intrauterine fetal retardation and obesity.

Then, the aim of this study was to identify proteins for which short-term abundance pattern in adipose tissues could have been altered by high protein intake in IUGR suckling piglets. In a

☆ This work was partly supported by the Agence Nationale de la Recherche (ANR-05-PNRA-09). Ousseynou Sarr was supported by a scholarship from INRA and the research fund of Region Bretagne (France).
☆☆ The authors have declared that no conflict of interest exists.
* Corresponding author. INRA, UMR1079 SENAH, Domaine de la Prise, 35590 Saint-Gilles, France. Tel.: +33 2 23 48 57 52; fax: +33 2 23 48 50 80.
E-mail address: Florence.gondret@rennes.inra.fr (F. Gondret).

0955-2863/$ - see front matter © 2012 Elsevier Inc. All rights reserved.
doi:10.1016/j.jnutbio.2011.09.002

complementary study, we have demonstrated lower tissue lipid content and depressed activities of lipogenic enzymes in perirenal and subcutaneous adipose tissues of those piglets compared with IUGR piglets fed adequate protein levels until weaning [14]. In the current study, the potential of 2DE-MS to reveal a global picture of the short-term adaptation of adipose tissues was evaluated in piglets subjected to IUGR followed by a high protein intake during sucking.

2. Materials and methods

2.1. Animals and diets

The care and use of piglets were performed in compliance with the guidelines of the French Ministry of Food, Agriculture and Fisheries. The scientific and technical staffs obtained an agreement from the French veterinary services to conduct animal research. The milk replacer powders were supplied by "la laiterie de Montaigu" (France). The current experiment is a subset of a larger study investigating the immediate and lasting effects of early high protein intakes on growth rate and adipose tissue phenotype [14]. Briefly, 10 crossbred full-term IUGR piglets (mean birth body weight of 0.92±0.02 kg, 10th percentile) were obtained from the experimental herd of INRA (Saint-Gilles, France). These piglets were allowed to suckle colostrum from their dams for the first 2 days. Pairs of littermates of the same sex were then randomly assigned to one of the two dietary groups (two entire males and three females in each group). They received milk replacers (Table 1) formulated to provide an adequate (AP, 1.05 g of protein/100 kJ mimicking sow's milk) or a high (HP, 1.5 g of protein/100 kJ) protein supply. After separation from their dam, they were placed individually in incubators (33°C, 60% humidity) and were bottle-fed every 2 h from 7:00 a.m. to 11:00 p.m. and once during the night at 3:00 a.m. from day 2 to day 7 [15]. At day 7, piglets were transferred into stainless steel metabolic cages in a temperature-controlled room (30°C), and they were then fed with an automatic formula feeder up to 28 days of age. The daily formula rations of piglets were calculated in net energy (NE) and were 1305 kJ per kg $BW^{0.75}$ during the whole experimental period. The HP powder was formulated to provide more protein and amino acids per NE than the AP powder, and the amount of proteins offered to the HP piglets was progressively increased to reach 41% more than AP intake from day 8 onwards. At day 28, experimental piglets (average body weight of 4.9 kg±0.2 kg and 5.5 kg±0.4 kg for AP and HP pigs, respectively) were sacrificed 90 min after the last meal at the experimental facilities of INRA (Saint-Gilles, France).

2.2. Sample collection and histological analyses

Adipose tissue at the perirenal location (PAT) was immediately removed and weighed, and a portion was prepared for later analysis. A sample of dorsal subcutaneous adipose tissue (SCAT) was also collected at the last rib level from the left half-carcass within 15 min after death. For histological analysis, samples of adipose tissue were restrained on flat sticks and frozen in isopentane cooled by liquid nitrogen. Other adipose tissue samples were cut into small pieces and frozen in liquid nitrogen. All samples were then stored at −75°C until analyses. Cross-sectional areas of adipocytes were measured from serial cross-sections of frozen PAT or SCAT cut in a cryostat, as previously described [14]. The distribution of adipocyte diameters (μm) into classes was then calculated.

2.3. Adipose tissue proteins solubilization

Frozen adipose tissue samples of approximately 150 mg were crushed with a mortar and a pestle under liquid nitrogen. They were homogenized with a Polytron grinder (Kinematica, Bioblock Scientific, Switzerland) in 1 ml of ice-cold lysis buffer (pH 7.4) containing 10 mmol/L Tris base, 1 mmol/L EDTA, 0.25 mol/L sucrose and compete protease inhibitors (Roche Diagnostics, GmbH, Mannheim, Germany). Homogenates were stirred for 1 h on ice using glass bead agitators (Heidolph, Germany) and were then centrifuged at 10 000*g* at 4°C for 15 min. The resulting supernatants (below the fat cake) contained soluble proteins. The total protein concentration of extracts was assessed by Bradford reagent (BioRad, Hercules, CA, USA) using bovine serum albumin as a standard [16]. The protein extracts were then stored at −75°C until use for later electrophoresis.

Table 1
Composition of AP and HP formula

Item	AP	HP
Protein, g/L	51.4	77.0
Lipid, g/L	82.0	79.0
Carbohydrates, g/L	49	46
Energy, kJ/L	4753	5030
Protein/energy, g/100 kJ	1.05	1.5

2.4. Two-dimensional gel electrophoresis

The 2DE analysis was performed on soluble protein extracts of the two experimental groups, thus allowing the majority of enzymes and some of the low-expressed proteins to be more easily studied. Unless indicated, all the materials used were supplied by GE Healthcare (Saclay, France). For the first dimension, soluble proteins (100 μg) were mixed with Destreack solution and 2% carrier ampholytes to make up the volume to 450 μl. Immobilized pH gradient (IPG) strips (24 cm, 3–10 pH nonlinear) were rehydrated passively with the protein extracts over a period of 16 h. Proteins were then isoelectrically focused on an Ettan IPGphorII system according to the following settings: 1 h at 120 V, 1 h at 200 V, 1 h at 500 V, 6 h at 1000 V, 1 h 30 min at 8000 V and a constant of 8000 V until approximately 48 000 Vh was reached. Subsequently, the IPG strips were equilibrated in two steps of 12 min each at room temperature with gentle agitation. The first equilibration solution contained 50 mmol/L of pH 8.8 Tris-HCl (Sigma) buffer, with 6 mol/L urea, 65 mmol/L dithiothreitol (DTT, Interchim, Montluçon, France), 2% sodium dodecyl sulfate (SDS) (v/w, Interchim) and 30% glycerol (v/v, Interchim). In the second equilibration solution, DTT was replaced by 4.5% iodoacetamide, and 0.03% bromophenol blue (Sigma) was added as a dye. Following equilibration, the strips were gently rinsed in water to remove buffer excess, then applied onto 12.5% SDS–polyacrylamide gel electrophoresis (PAGE) gels and sealed with 0.5% agarose solution. The SDS-PAGE was conducted in a vertical Ettan DALTsix system. A power of 5 W per gel was applied for 45 min, and a power of 17 W per gel was then applied until the bromophenol blue dye front reached the bottom of the gels. Proteins were then visualized by sensitive silver staining [17]. In PAT and SCAT, respectively, the gel with the best resolution and the greatest number of detected spots was used as a master gel for image analysis. Finally, two preparative gels per tissue were made by pooling an equal volume of each extract (200 μg and 400 μg of all protein extracts, respectively) and stained [18] to allow spot picking and further MS identification.

2.5. Image analysis

The gels were immediately scanned with an UMAX ImageScanner (GE Healthcare) at 200 dpi and analyzed by Melanie 7.0 software (GeneBio, Switzerland). A total of 20 analytical 2DE gels were considered with two match sets constructed for the two kinds of adipose tissues. For each match set, two subsequent match sets were built based on the dietary experimental piglet groups (HP and AP) consisting each of five biological replicates. The process of automatic spot matching was done using the master gel as reference both within and between submatch sets. Manual fine editing matching was performed when necessary. The volume of each spot was normalized by dividing its volume by the total volume of all spots in the gel (outliers being removed) to take into account variations due to protein loading and staining. Only spots detected in a minimum of $n-1$ biological replicates from the two submatch sets were considered. The results were expressed according to fold-change value, which represents the expression ratio of the HP group to the AP group. Ratios of abundance of protein spots in HP group relative to AP group are inversed and are preceded by a minus sign for value less than 1.

2.6. Protein identification

Protein spots of interest were manually cut out of the gels using pipette tips. Gel pieces were placed into a 1.5-ml microcentrifuge tube in a solution of 1% acetic acid (Carlo Erba, Val de Reuil, France). Excised spots were processed and digested with trypsin as described previously [19]. Extraction was performed in two successive steps by adding 50% v/v acetonitrile (ACN)/0.1% trifluoric acid (TFA). Digests were dried out and dissolved with 2 mg/ml alpha-cyano-4-hydroxycinnamic acid in 70% ACN/0.1% TFA before spotting onto targets (384 Scout MTP 600 μm AnchorChip, Bruker Daltonik, Bremen, Germany). The peptide fragments produced from each protein spot were used to generate peptide fragment mass data via matrix-assisted laser desorption/ionization–time of flight (TOF)/TOF mass spectrometry analysis (Ultraflex, Bruker Daltonik). The peptide fragment mass data were processed with the FlexAnalysis software (V2.2, Bruker Daltonik). All analyses were performed on the Proteomics Core Facility of Biogenouest (Rennes, France). Autolysis products of trypsin were used for internal calibration. The monoisotopic masses of tryptic peptides were used to query NCBI nonredundant sequences databases of all mammalian proteins using the MASCOT search engine (http://www.matrixscience.com). The mass tolerance was set at 100 ppm for the parent ion and at 0.5 Da for the fragment ions. To avoid incorrect identifications, four matched peptides per protein were required at least, and each matching was carefully checked manually by considering MASCOT probabilistic score and accuracy of the experimental to theoretical isoelectric point and molecular weight.

2.7. Protein categorization

Identified proteins were functionally classified according to their biological process terms provided in Gene Ontology Consortium (http://www.ncbi.nlm.nih.gov/gene) for *Homo sapiens* and considering eventually their parent terms (http://amigo.geneontology.org).

2.8. Western blotting

To confirm our findings with 2DE, Western blotting was performed for annexin 2 protein. Soluble proteins of individual samples of SCAT and PAT from the two dietary groups were subjected to one-dimensional SDS-PAGE (10%) and transferred onto polyvinylidene fluoride membranes (Bio-Rad, Marnes-la-Coquette, France). The membranes were blocked with Tris-buffered saline (TBS; 50 mmol/L Tris-HCl pH 8.6, 150 mmol/L NaCl, 0.1% Tween) containing 5% nonfat dry milk (Bio-Rad). The blots were incubated in TBS/0.1% Tween for 1 h at room temperature with a primary antibody against annexin 2 (sc-30757; Santa Cruz Biotechnology; final dilution of 1/500) or a primary antibody against β-actin (A-5316; Sigma; final dilution 1/5000), respectively. Thereafter, blots were washed in 0.1% Tween/TBS and incubated at room temperature for 1 h with secondary horseradish-peroxidase-conjugated antibody (1/5000) raised against goat IgG (Santa Cruz Biotechnology). Protein bands were visualized by the ECL Western Blotting detection reagents (GE Healthcare). The chemiluminescence signal was captured with a Luminescent Image Analyzer (GE Healthcare), and densitometric values (arbitrary units) were determined using the ImageQuant LAS 4000 software (GE Healthcare). The abundance of annexin 2 was expressed relatively to β-actin protein amount in each sample.

2.9. Quantitative real-time reverse transcriptase polymerase chain reaction

Frozen samples of PAT or SCAT (80–100 mg each) were homogenized in 1 ml of Trizol (Invitrogen, Cergy-Pontoise, France) using a TissueLyser (Qiagen, Haan, Germany). Homogenates were then treated according to the manufacturer's instructions. RNA was finally purified using the NucleoSpin RNA II kit (Macherey-nagel, Hoerdt, France). The quantification of RNA was performed by spectrophotometry (NanoDrop, Thermofisher Scientific, Illkirch, France). The integrity of RNA was assessed using the Agilent RNA 6000 Nano kit (Agilent Technologies, Merignac, France) with an Agilent 2100 Bioanalyzer (Agilent Technologies). Treated-DNAse total RNA (2 μg) was reverse-transcribed using High Capacity cDNA Reverse Transcription kit (Applied Biosystems, Courtaboeuf, France). Quantitative real-time quantitative polymerase chain reaction (qPCR) analyses were performed with 5 ng of reverse-transcribed RNA using SYBR Green I reagents (Applied Biosystems) in a StepOnePlus RT-qPCR System instrument with the fast mode (Applied Biosystems). The primers (Table 2) were designed from porcine sequences using Primer Express software 3.0 (Applied Biosystems). Forty cycles of amplification were performed, with each cycle consisting of denaturation at 95°C for 15 s and hybridization and extension at 60°C for 1 min. An internal calibrator (pool of total RNA reverse-transcribed from all adipose tissue samples) and negative controls were used for each run of qPCR. Quantification cycle values (C_q, corresponding to the number of cycles at half of the exponential phase of the curve of the qPCR reaction) are means of duplicate measurements. ΔC_q for each gene was calculated as the difference in C_q values derived from the duplicated samples and the internal calibrator. Amplification efficiency (E) of the qPCR reaction was determined for each target using standard curves generated with decreasing concentration of cDNA samples (16 ng to 0.0039 ng) and calculated as $E=10^{(1/\text{slope})}$. The transcript levels of target genes were normalized to the transcript level of *HPRT1* housekeeping gene. The relative gene expression was expressed as follows: $E^{-\Delta C_q^{\text{target gene}}}/E^{-\Delta C_q^{HPRT1\ \text{gene}}}$.

2.10. Statistical analysis

The differential abundances of the protein spots were analyzed by analysis of variance (ANOVA) with the fixed effects of dietary group (AP, HP) using Melanie 7.0 software (GeneBio). Only protein spots with at least a |1.2|-fold between HP and AP dietary groups were considered as biologically relevant in each adipose tissue. Other data were processed by ANOVA using the General Linear Model of SAS (SAS Institute, Cary, NC, USA) with dietary group (HP or AP) as the main effect. Values are given as means±standard error (S.E.M.). Differences between dietary groups were considered significant at $P<.05$, whereas $0.05<P<.10$ was discussed as a trend.

3. Results

3.1. Histological characteristics of adipose tissues

The two adipose tissues of 28-day-old HP piglets exhibited greater proportions of small adipocytes (diameter <25 μm in PAT and diameter <35 μm in SCAT, respectively) and, conversely, lower proportions of large adipocytes (diameter >45 μm in PAT and diameter >55 μm in SCAT, respectively) when compared with adipose tissues of AP piglets (Fig. 1). Therefore, mean adipocyte diameters were lower in the two fat pads of HP piglets compared with AP ones at day 28 (data not shown).

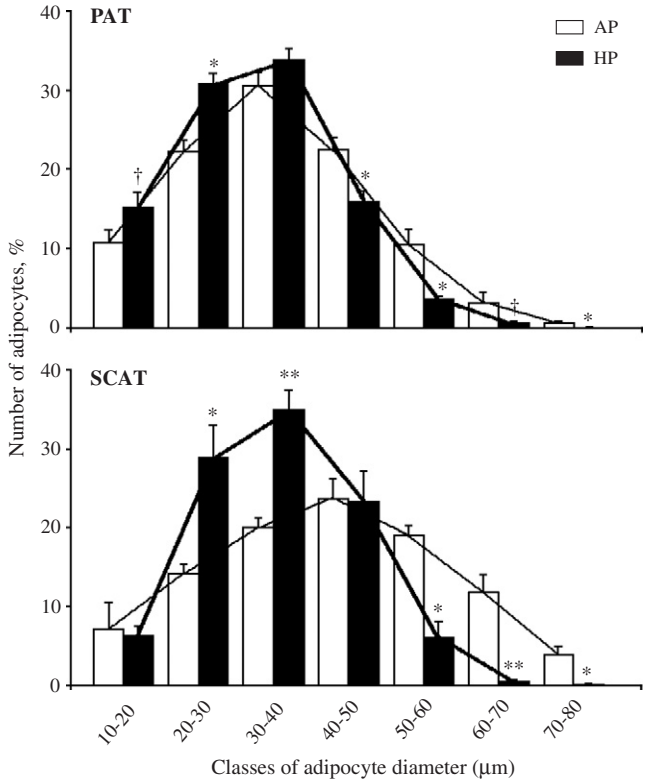

Fig. 1. Frequencies of diameter classes of PAT and SCAT of 28-day-old piglets fed AP or HP neonatal formula. Adipocyte cross-sectional areas were obtained from histological slides of frozen adipose tissues of the two groups ($n=5$ piglets per group), and diameters were calculated assuming adipocytes as spheres. $^{**}P\leq.01$; $^{*}P\leq.05$; $^{\dagger}P\leq.10$ for HP vs. AP groups.

3.2. High protein intake and adipose tissue proteome

About 900 to 1300 spots were automatically detected on the gels for PAT and SCAT, respectively, from which about 60% were successfully matched between the gels. A total of 257 spots to 517 spots for PAT and SCAT, respectively, were repeatedly present in the gels and were thus considered for differential analysis.

A total of 32 spots displayed an altered abundance between HP and AP piglets. Among them, 13 protein spots differed in their ratio of abundance ($P<.05$: 3 spots in PAT, 10 spots in SCAT), and 19 spots tended to be modified ($P<.10$: 4 spots in PAT, 15 spots in SCAT). Eighteen spots corresponding to 15 unique proteins were successfully identified by mass spectrometry (rate of identification: 56%). The positions of the identified protein spots are indicated in the two

Table 2
Primer sequences of selected genes

Gene	Accession number	Primers
Annexin A1	X95108	Sense: 5′-TGCTAAGGGTGACCGATCTGA-3′ Antisense: 5′-TCATATAAAGCCCTTGCATCTGTATC-3′
Annexin A2	AY706383	Sense: 5′-AACTTTGATGCTGAGCGAGATG-3′ Antisense: 5′-GACCTCGTCCACACCTTTGG-3′
Hypoxanthine phosphoribosyltransferase 1	DQ845175	Sense: 5′-TACCTAATCATTATGCCGAGGATTT-3′ Antisense: 5′-AGCCGTTCAGTCCTGTCCAT-3′

representative 2DE gels for perirenal (Fig. 2A) and subcutaneous (Fig. 2B) locations. Those protein spots belong to various pathways as indicated by GO annotation category (Table 3), such as cell organization and regulation of cell cycle and apoptosis, protein complex assembly and protein catabolic process, metabolic processes for carbohydrates or amino acids, cell redox homeostasis and nucleotide biosynthesis.

Notably, the phospholipid binding protein annexin 2 tended to be expressed ($P<.10$) with a lower abundance in both PAT and SCAT of the HP piglets compared with the AP ones. The abundance of annexin 1, another type of annexin, also tended to be lower in HP piglets than in AP ones, but only for PAT. Moreover, guanine nucleotide binding protein-like 3 (*GNL3L*) that is essential for ribosomal pre-rRNA processing and cell proliferation also tended to have a lower abundance in PAT of HP piglets compared with AP piglets. Conversely, intracellular actin-modulating protein cofilin-1 and dynactin binding to intracellular microtubules, two proteins that might be involved in antiapoptosis or cell death, respectively, exhibited a greater abundance ($P<.05$) in HP piglets compared with AP piglets, but only in SCAT. In addition, cyclophilin-A (peptidyl-prolyl *cis-trans* isomerase A) had a greater abundance ($P<.05$) in the same tissue of HP piglets compared with AP ones. The dietary-associated changes in proteins linked to metabolic processes concerned mainly SCAT. Ribose-5-phosphate isomerase participating in the pentose-phosphate shunt had a greater abundance ($P=.05$) in HP piglets than in AP piglets, whereas lactate dehydrogenase (LDH), an enzyme involved in glucose anaerobic pathway, tended to be lower in SCAT of HP piglets compared with AP animals. Two isoforms of glutamate dehydrogenase 1 (GLUD1), an enzyme involved in cellular amino acid (glutamate) catabolic process, were or tended also to be less abundant in SCAT of HP piglets compared with AP piglets. The *26S* protease regulatory

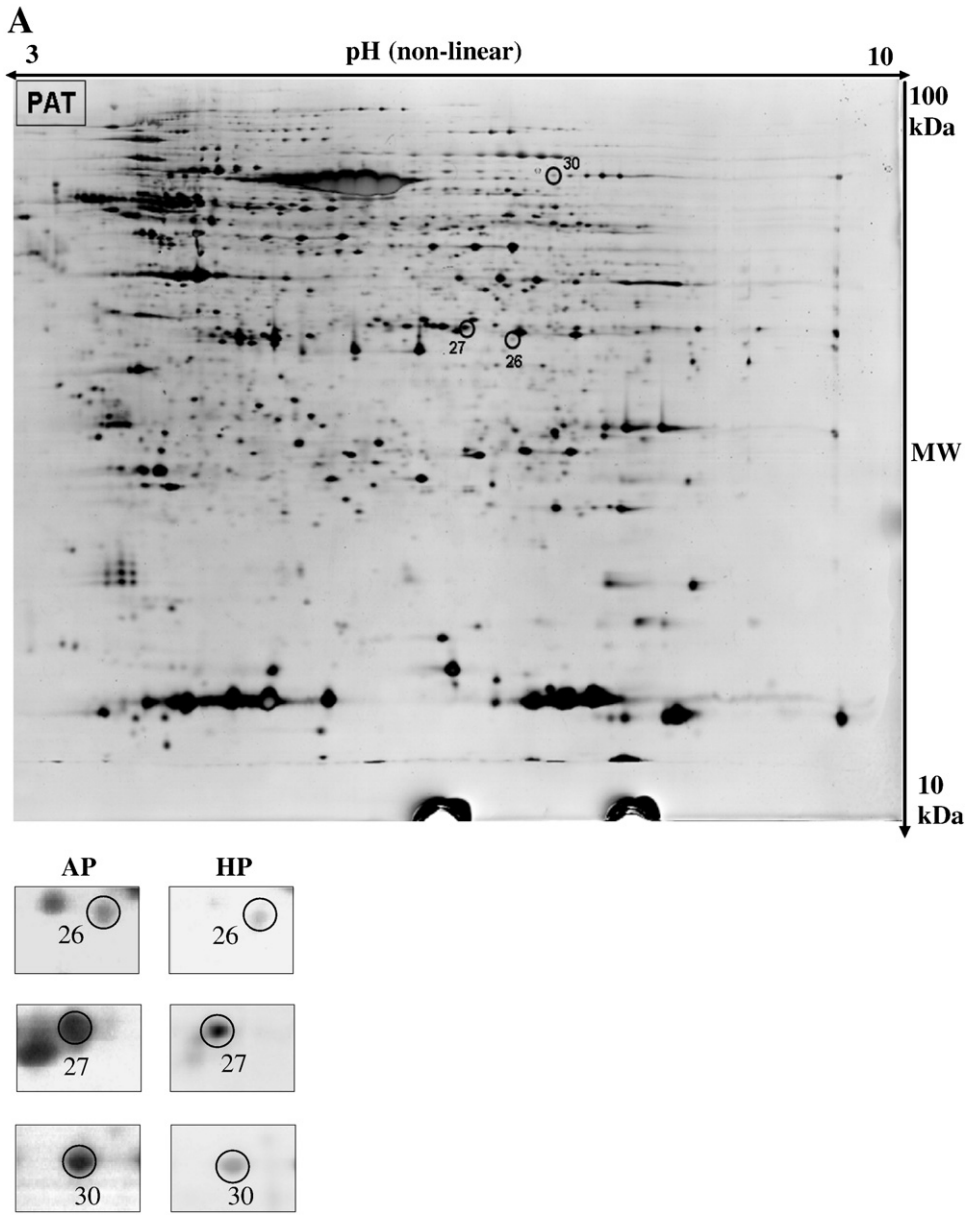

Fig. 2. Location of identified protein spots having a differential abundance in (A) PAT and (B) SCAT between 28-day-old piglets fed AP or HP neonatal formula. For each adipose tissue site, soluble protein extracts ($n=5$ piglets per group) were subjected to 2DE followed by sensitive silver staining. A representative gel in each adipose tissue is shown, together with the close-up sections of identified differentially expressed protein spots in AP vs. HP piglets. Corresponding spot numbering is listed in Table 3.

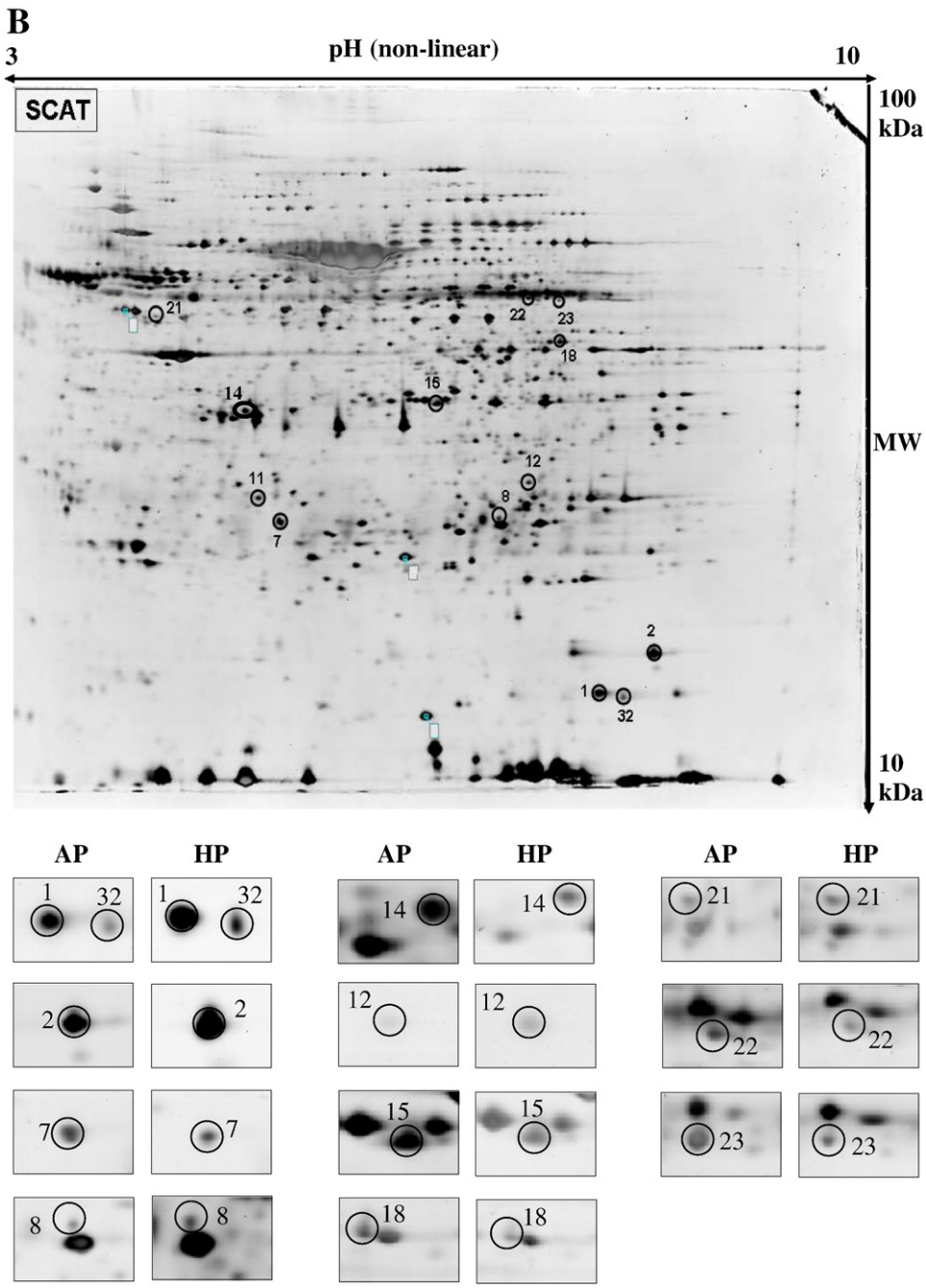

Fig. 2 (*continued*).

subunit 8 participating in the complex-dependent proteasomal protein degradation process tended to have a lower abundance in SCAT of HP piglets. Finally, trends were observed ($P<.10$) for a greater abundance of glutathione *S*-transferase omega 1 (GSTO1) belonging to the multigene family of detoxification enzymes in SCAT of piglets fed HP formula, whereas a lower abundance in peroxiredoxin 6 (PRDX6) involved in the response to oxidative was noticed in the formers compared with AP piglets.

3.3. High-protein formula and annexin expressions

Changes in abundance of annexins in the two adipose tissues were further studied by target methodologies. The results of annexin 2 blots (Fig. 3) confirm the results of the 2DE analysis. The concentration of annexin 2 protein was significantly lower (1.5-fold to 2.5-fold; $P<.05$) in PAT and SCAT of HP piglets compared with AP ones. On the contrary, mRNA levels of *ANXA1* and *ANAX2* genes did not differ between HP and AP groups whatever the adipose tissue (Table 4).

4. Discussion

The current study reports little changes occurring in adipose tissue proteomes of IUGR animals fed an HP formula during the neonatal period. The number of protein spots identified is however in the range observed in other models of IUGR neonatal piglets for adipose tissue [12] and tissues other than fat pads [13]. It is also in agreement with

Table 3
Differentially expressed proteins in PAT and SCAT from 28-day-old piglets fed AP or HP formula between 2 and 28 days of age

Spot	Protein name[a]	Swiss-Prot accession	Species	pI[a]	MW[a] (kDa)	Sequence coverage,[b] %	MASCOT score[c]	SCAT HP/AP[d]	PAT HP/AP[d]	*P* value[d]
Positive regulation of binding										
15	Annexin 2 (*ANXA2*)	P19620	*Sus scrofa*	6.6	38.5	60.2	170	−2.0		.074
26	Annexin 2 (*ANXA2*)	P19620	*S. scrofa*	6.6	38.5	51.0	98.5		−2.2	.097
Cell cycle, antiapoptosis										
27	Annexin 1 (*ANXA1*)	P19619	*S. scrofa*	6.5	38.7	35.8	106		−1.8	.080
21	Dynactin subunit 2 (*DCTN2*)	Q13561	*H. sapiens*	5.0	44.2	36.2	123	+2.5		.007
2	Cofilin-1 (*CFL1*)	P10668	*S. scrofa*	9.1	18.5	56.0	80	+2.3		.023
Protein complex assembly, protein folding										
32	Peptidyl-prolyl *cis-trans* isomerase A–cyclophilin-A (*PPIA*)	P62936	*S. scrofa*	9.4	17.9	62.2	82	+2.1		.018
18	26S protease regulatory subunit 8 (*PSMC5*)	P62197	*Rattus norvegicus*	7.8	45.6	39.2	70	−2.7		.089
Metabolic process: pentose-phosphate shunt										
8	Ribose-5-phosphate isomerase (*RPIA*)	A2TLM1	*S. scrofa*	9.4	32.7	41.5	75	+2.0		.056
Metabolic process: carbohydrate metabolic process										
14	L-lactate dehydrogenase A chain (*LDHA*)	Q9W7L5	*Sceloporus undulatus*	8.0	36.6	34.6	82	−2.0		.064
Metabolic process: amino acid metabolism										
22	Glutamate dehydrogenase 1, mitochondrial (*GLUD1*)	P00366	*Bos taurus*	7.8	61.5	28.7	79	−1.7		.021
23	Glutamate dehydrogenase 1, mitochondrial (*GLUD1*)	P00367	*H. sapiens*	8.5	61.4	42.0	146	−1.6		.078
Metabolic process: cell redox homeostasis										
7	Peroxiredoxin 6 (*PRDX6*)	Q9TSX9	*S. scrofa*	5.7	25.0	75.0	182	−1.4		.071
12	Glutathione *S*-transferase omega 1 (*GSTO1*)	Q9N1F5	*S. scrofa*	7.6	27.4	42.3	77	+1.9		.081
Metabolic process: nucleotide biosynthesis										
1	Nucleoside diphosphate kinase B (*NME2*)	Q2EN76	*S. scrofa*	9.0	17.2	73.7	112	+2.6		.026
Cell component biogenesis: ribosome biogenesis										
30	Guanine nucleotide-binding protein-like 3-like protein (*GNL3L*)	Q3T0J9	*B. taurus*	9.6	64.8	22.3	72		−2.1	.091

Data corresponded to $n=5$ individual extracts in each dietary groups.
[a] Protein name was indicated together with official symbol of the corresponding human gene ortholog into brackets. Molecular weight (MW) and isoelectric point (pI), theoretical (from NCBI database).
[b] Total percentage of sequence coverage.
[c] The score obtained from the database search using the MASCOT program (Matrix Science, www.matrixscience.com).
[d] Ratio of protein abundance in SCAT or PAT from HP group relative to AP group and associated *P* value. Ratios are inversed and are preceded by a minus sign for value less than 1.

the number of spots showing a differential abundance with rapid vs. slow catch-up growth in IUGR rats during suckling [20].

The dietary-affected protein spots were found in a greater number in SCAT than in PAT of experimental piglets in the current study. This could reflect differences in the developmental patterns of these two adipose tissues in the pig [21] that may cause adipose tissues proteomes to respond differently to early dietary interventions. Moreover, the proteins identified after 2DE analysis provide an additional picture of the way by which IUGR piglets adapt to the HP formula during sucking. Especially, a depressed abundance of annexin 2 was observed at both PAT and SCAT locations in HP piglets, whereas the trend for a lower abundance of annexin 1 in the HP group with the AP compared was limited to PAT. Small adipocytes generally display a lower abundance in annexin 2 compared with large adipocytes in mice [22]. Therefore, the report of a lower abundance of annexin 2 in adipose tissues of HP piglets agrees with the smaller diameter of adipocytes found in the two fat pads of HP compared with AP piglets. In addition, an attractive functional proposal for annexin 2 includes the regulation of membrane trafficking and exocytosis [23], such as insulin-stimulated translocation of the glucose transporter GLUT4 in differentiated adipocytes [24]. A down-regulation in the expression levels of glucose transporters GLUT1 *(SLC2A1)* and GLUT4 *(SLC2A4)* has been reported at both PAT and SCAT locations for HP piglets compared with AP piglets in our complementary study [14]. The lower abundance in annexin 2 in response to HP formula may thus have additional effects on glucose uptake in adipocytes in each site. Conversely, annexin 1 has been suggested to alter the sensitivity of adipose tissue to catecholamines, thereby modulating lipolysis in mice [25]. Because the expression levels of genes encoding two lipolytic enzymes were lower after HP feeding only at PAT location in our complementary study [14], it is then tempting to speculate that

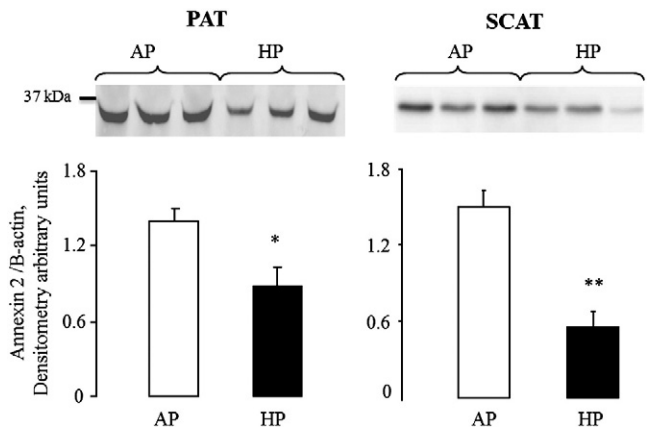

Fig. 3. Target analyses of annexin 2 abundance in perirenal fat or subcutaneous fat of 28-day-old piglets fed AP or HP neonatal formula. Representative Western blots of annexin 2 are shown, together with relative densitometric values of protein band of annexin 2 relative to internal standard β-actin. Values are means±S.E.M. Significance of differences between HP and AP groups ($n=5$ piglets in each group): $^{*}P<.05$; $^{**}P<.01$.

Table 4
Expression levels of annexins in adipose tissue of experimental pigs

	SCAT			PAT		
	HP	AP	*P* value	HP	AP	*P* value
Gene[a]						
ANAX1	0.62±0.07	0.69±0.11	.625	0.58±0.04	0.60±0.09	.837
ANAX2	0.42±0.05	0.44±0.03	.846	0.62±0.05	0.69±0.02	.647

[a] mRNA level (mean + sem) of the target gene relative to *HPRT1* expression in SCAT or PAT.

the lower abundance in annexin 1 in PAT of HP piglets could have contributed to an attenuated lipolytic ability in those piglets compared with AP piglets. Finally, the absence of variation in *ANXA1* and *ANXA2* mRNA levels in adipose tissues of experimental piglets suggests an adaptation to HP formula at the posttranscriptional level, a pattern of response that has been previously shown for annexins in human adipose tissue after insulin sensitization [26]. However, since we were not able to directly measure glucose uptake and fatty acid release in this experiment, further analyses should be undertaken to explore the molecular targets and pathways associated with annexins modulation in isolated porcine adipocytes.

In SCAT of HP piglets, we observed a greater abundance of the ribose-5-phosphate isomerase (*RPIA*), an enzyme involved in the nonoxidative branch of the pentose-phosphate pathway in cells. The main function of this metabolic route is to produce ribose-5-phosphate that represents the sugar component of RNA playing roles in dividing cells; however, a redirection of the carbohydrates flux from glycolysis to the pentose-phosphate pathway is also observed during oxidative stress [27]. A number of dietary-altered proteins in the current study could then sign for response mechanisms to counteract oxidative stress in adipose tissues of HP piglets. The omega class protein of the cytosolic glutathione *S*-transferase superfamily, which is an enzyme that catalyzes reduction reactions to act for detoxification mechanisms and to mitigate oxidative stress [28], was found with a greater abundance in SCAT of HP piglets. On the contrary, peroxiredoxin 6, which is involved in stress response [29], had a lower abundance in SCAT of those piglets compared with AP piglets. Moreover, the chaperone protein cyclophilin-A had a greater abundance in SCAT of HP piglets; this protein protects cells against oxidative stress by conferring some resistance to the peroxides [30]. Finally, as reported in a yeast model in response to oxidative stress [31], glutamate dehydrogenase was found with a lower abundance in HP adipose tissue compared with AP piglets. However, the biological significance of this dietary-induced modulation needs to be further assessed in pig adipose tissue. Indeed, this first central enzyme in glutamate metabolism could also participate in fatty acid synthesis through the backward pathway of the Krebs cycle as shown in human adipose tissue [32,33]. Together, these changes may indicate a reduced level of oxidative stress inside the adipocytes of sucking piglets fed HP formula or could simply reflect the inflammatory status of adipose tissue. First, many antioxidant defense enzymes depend on macronutrients such as proteins, which were provided in excess by the HP formula. Second, detoxification markers such as glutathione transferase are found to be moderately enhanced in the liver of weaned rats fed a high-protein diet to induce a sharp reduction in their adipose tissue [34]; moreover, adequate protein feeding may induce oxidative stress compared with a high protein intake in adult rats [35]. In this regard, prior reports in IUGR pig neonates have suggested oxidative stress in those piglets compared with normal-sized littermates [13]. Therefore, it remains to be assessed whether feeding HP formula during sucking may stimulate defense mechanisms against oxidative stress in IUGR piglets that might be helpful during their later life.

Finally, two proteins involved in cytoskeleton rearrangement (dynactin and cofilin-1) were found to be more abundant in SCAT of HP piglets. Non-muscle-type cofilin controls the mechanical tension of cell by regulating actin polymerization and participates thereby in differentiation and lipid accumulation in adipocytes [36,37]. Dynactin is one of the proteins that facilitate bidirectional movements of individual organelles such as lipid droplets in microtubules [38]. This suggests that cell cytoskeleton remodeling could be an additional mechanism accounting for reduced lipid accumulation and lower adipose tissue weight [39] in HP piglets.

In conclusion, although the current proteomic approach could be judged somewhat disappointing, it matches with our recent work showing little changes in expression levels of adipose genes in response to HP formula [14] despite clear reductions in their adiposity at 28 days of age. Together, these results suggest that the HP formula may act simply to slow down the catch-up fat growth that naturally occurs in IUGR piglets during sucking period [10], without drastic changes in adipocyte physiology.

Acknowledgments

We wish to thank C. Tréfeu for her expert technical assistance. We acknowledge all the staff involved in the animal care and feeding as well as G. Savary for the maintenance of incubators and automatic formula feeders. The authors also thank E. Com (High-Throughput Proteomics Platform of Biogenouest, 263 Avenue du Général Leclerc, Bâtiment 24, Campus de Beaulieu, Rennes, 35042, France) for assistance during mass spectrometry identification.

References

[1] Bruce KD, Hanson MA. The developmental origins, mechanisms, and implications of metabolic syndrome. J Nutr 2010;140:648–52.
[2] Barker DJ, Hales CN, Fall CH, Osmond C, Phipps K, Clark PM. Type 2 (non-insulin-dependent) diabetes mellitus, hypertension and hyperlipidaemia (syndrome X): relation to reduced fetal growth. Diabetologia 1993;36:62–7.
[3] Hales CN, Barker DJ. The thrifty phenotype hypothesis. Br Med Bull 2001;60:5–20.
[4] Premji SS, Fenton TR, Sauve RS. Higher versus lower protein intake in formula-fed low birth weight infants. Cochrane Database Syst Rev 2006;25:CD003959.
[5] Ziegler EE. Growth of breast-fed and formula-fed infants. Nestle Nutr Workshop Ser Pediatr Programme 2006;58:51–63.
[6] Rolland-Cachera MF, Deheeger M, Akrout M, Bellisle F. Influence of macronutrients on adiposity development: a follow up study of nutrition and growth from 10 months to 8 years of age. Int J Obes Relat Metab Disord 1995;19:573–8.
[7] Scaglioni S, Verduci E, Fiori L, Lammardo AM, Rossi S, Radaelli G, et al. Body mass index rebound and overweight at 8 years of age in hyperphenylalaninaemic children. Acta Peadiatr 2004;93:1596–600.
[8] Koletzko B. Long-term consequences of early feeding on later obesity risk. In protein and energy requirements in infancy and childhood. Nestle Nutr Workshop Ser Pediatr Program 2006;58:1–18.
[9] Fox CS, Massaro JM, Hoffmann U, Pou KM, Maurovich-Horvat P, Liu CY, et al. Abdominal visceral and subcutaneous adipose tissue compartments: association with metabolic risk factors in the Framingham Heart Study. Circulation 2007;116:39–48.
[10] Morise A, Sève B, Macé K, Magliola C, Le Huërou-Luron I, Louveau I. Impact of intrauterine growth retardation and early protein intake on growth, adipose tissue, and the insulin-like growth factor system in piglets. Pediatr Res 2009;65:45–50.
[11] Des Robert C, Li N, Caicedo R, Frost S, Lane R, Hauser N, et al. Metabolic effects of different protein intakes after short term undernutrition in artificially reared infant rats. Early Hum Dev 2009;85:41–9.
[12] Sarr O, Louveau I, Kalbe C, Metges CC, Rehfeldt C, Gondret F. Prenatal exposure to maternal low or high protein diets induces modest changes in the adipose tissue proteome of newborn piglets. J Anim Sci 2010;88:1626–41.
[13] Wang J, Chen L, Li D, Yin Y, Wang X, Li P, et al. Intrauterine growth restriction affects the proteomes of the small intestine, liver, and skeletal muscle in newborn pigs. J Nutr 2008;138:60–6.
[14] Sarr O, Gondret F, Jamin A, Le Huërou-Luron I, Louveau I. A high-protein neonatal formula induces a temporary reduction of adiposity and changes later adipocyte physiology. Am J Physiol Reg Integr Comp Physiol 2011;300:R387–97.
[15] Jamin A, D'Inca R, Le Floc'h N, Kuster A, Orsonneau JL, Darmaun D, et al. Fatal effects of a neonatal high-protein diet in low-birth-weight piglets used as a model of intrauterine growth restriction. Neonatology 2010;97:321–8.
[16] Bradford MM. A rapid and sensitive method for the quantitation of microgram quantities of protein utilizing the principle of protein-dye binding. Anal Biochem 1976;72:248–54.
[17] Blum H, Beier H, Gross HJ. Improved silver staining of plant proteins, RNA and DNA in polyacrylamide gels. Electrophoresis 1987;8:93–9.
[18] Shevchenko A, Wilm M, Vorm O, Mann M. Mass spectrometric sequencing of proteins from silver-stained polyacrylamide gels. Anal Chem 1995;68:850–8.
[19] Rolland AD, Evrard B, Guitton N, Lavigne R, Calvel P, Couvet M, et al. Two-dimensional fluorescence difference gel electrophoresis analysis of spermatogenesis in the rat. J Proteome Res 2007;6:683–97.
[20] Alexandre-Gouabau MC, Bailly E, Moyon TL, Grit IC, Coupé B, Le Drean G, et al. Postnatal growth velocity modulates alterations of proteins involved in metabolism and neuronal plasticity in neonatal hypothalamus in rats born with intrauterine growth restriction. J Nutr Biochem 2011, doi:10.1016/j.jnutbio.2010.11.008.
[21] Ramsay TG, Stoll MJ, Caperna TJ. Adipokine gene transcription level in adipose tissue of runt piglets. Comp Biochem Physiol B Biochem Mol Biol 2010;155:97–105.

[22] Blüher M, Wilson-Fritch L, Leszyk J, Laustsen PG, Corvera S, Kahn CR. Role of insulin action and cell size on protein expression patterns in adipocytes. J Biol Chem 2004;279:31902–9.
[23] Harder T, Gerke V. The subcellular distribution of early endosomes is affected by the annexin II2p11(2) complex. J Cell Biol 1993;123:1119–32.
[24] Huang J, Hsia SH, Imamura T, Usui I, Olefsky JM. Annexin II is a thiazolidinedione-responsive gene involved in insulin-induced glucose transporter isoform-4 translocation in 3T3-L1 adipocytes. Endocrinology 2004;145:1579–86.
[25] Warne JP, John CD, Christian HC, Morris JF, Flower RJ, Sugden D, et al. Gene deletion reveals roles for annexin A1 in the regulation of lipolysis and IL-6 release in epididymal adipose tissue. Am J Physiol Endocrinol Metab 2006;291:1264–73.
[26] Ahmed M, Neville MJ, Edelmann MJ, Kessler BM, Karpe F. Proteomic analysis of human adipose tissue after rosiglitazone treatment shows coordinated changes to promote glucose uptake. Obesity 2010;18:27–34.
[27] Wamelink MM, Struys EA, Jakobs C. The biochemistry, metabolism and inherited defects of the pentose phosphate pathway: a review. J Inherit Metab Dis 2008;31:703–17.
[28] Board PG. The omega-class glutathione transferases: structure, function, and genetics. Drug Metab Rev 2011;43:226–35.
[29] Simeone M, Phelan SA. Transcripts associated with Prdx6 (peroxiredoxin 6) and related genes in mouse. Mamm Genome 2005;16:103–11.
[30] Doyle V, Virji S, Crompton M. Evidence that cyclophilin-A protects cells against oxidative stress. Biochem J 1999;341:127–32.
[31] Godon C, Lagniel G, Lee J, Buhler JM, Kieffer S, Perrot M, et al. The H2O2 stimulon in Saccharomyces cerevisiae. J Biol Chem 1998;273:22480–9.
[32] Belfiore F, Iannello S. Fatty acid synthesis from glutamate in the adipose tissue of normal subjects and obese patients: an enzyme study. Biochem Mol Med 1995;54:19–25.
[33] Collins JM, Neville MJ, Pinnick KE, Hodson L, Ruyter B, van Dijk TH, et al. De novo lipogenesis in the differentiating human adipocyte can provide all fatty acids necessary for maturation. J Lipid Res 2011;52:1683–92.
[34] Lacroix M, Gaudichon C, Martin A, Morens C, Mathé V, Tomé D, et al. A long-term high-protein diet markedly reduces adipose tissue without major side effects in Wistar male rats. Am J Physiol Regul Integr Comp Physiol 2004;287:R934–42.
[35] Petzke KJ, Elsner A, Proll J, Thielecke F, Metges CC. Long-term high protein intake does not increase oxidative stress in rats. J Nutr 2000;130:2889–96.
[36] Choi KC, Roh SG, Hishikawa D, Miyahara H, Kuno M, Tsuzuki H, et al. Differential expression of the non-muscle cofilin gene between subcutaneous and visceral adipose tissue. Biosci Biotechnol Biochem 2003;67:2262–5.
[37] DeLany JP, Floyd ZE, Zvonic S, Smith A, Gravois A, Reiners E, et al. Proteomic analysis of primary cultures of human adipose-derived stem cells. Mol. Cell. Proteomics 2005;4:731–40.
[38] Valetti C, Wetzel DM, Schrader M, Hasbani MJ, Gill SR, Kreis TE, et al. Role of dynactin in endocytic traffic: effects of dynamitin overexpression and colocalization with CLIP-170. Mol Biol Cell 1999;10:4107–20.
[39] Higami Y, Barger JL, Page GP, Allison DB, Smith SR, Prolla TA, et al. Energy restriction lowers the expression of genes linked to inflammation, the cytoskeleton, the extracellular matrix, and angiogenesis in mouse adipose tissue. J Nutr 2006;136:343–52.